OPEN ACCESS Freely available online

PLoS one

Recombinant Lysyl Oxidase Propeptide Protein Inhibits Growth and Promotes Apoptosis of Pre-Existing Murine Breast Cancer Xenografts

Manish V. Bais[1], Matthew A. Nugent[2], Danielle N. Stephens[1], S. Selva Sume[1], Kathrin H. Kirsch[2], Gail E. Sonenshein[3], Philip C. Trackman[1,2]*

1 Division of Oral Biology, Boston University Henry M. Goldman School of Dental Medicine, Boston, Massachusetts, United States of America, **2** Department of Biochemistry, Boston University School of Medicine, Boston, Massachusetts, United States of America, **3** Department of Biochemistry, Tufts University School of Medicine, Boston, Massachusetts, United States of America

Abstract

Lysyl oxidase propeptide (LOX-PP) ectopic overexpression inhibits the growth of cancer xenografts. Here the ability and mode of action of purified recombinant LOX-PP (rLOX-PP) protein to inhibit the growth of pre-existing xenografts was determined. Experimental approaches employed were direct intratumoral injection (i.t.) of rLOX-PP protein into murine breast cancer NF639 xenografts, and application of a slow release formulation of rLOX-PP implanted adjacent to tumors in NCR nu/nu mice (n = 10). Tumors were monitored for growth, and after sacrifice were subjected to immunohistochemical and Western blot analyses for several markers of proliferation, apoptosis, and for rLOX-PP itself. Direct i.t. injection of rLOX-PP significantly reduced tumor volume on days 20, 22 and 25 and tumor weight at harvest on day 25 by 30% compared to control. Implantation of beads preloaded with 35 micrograms rLOX-PP (n = 10) in vivo reduced tumor volume and weight at sacrifice when compared to empty beads ($p<0.05$). A 30% reduction of tumor volume on days 22 and 25 ($p<0.05$) and final tumor weight on day 25 ($p<0.05$) were observed with a reduced tumor growth rate of 60% after implantation. rLOX-PP significantly reduced the expression of proliferation markers and Erk1/2 MAP kinase activation, while prominent increases in apoptosis markers were observed. rLOX-PP was detected by immunohistochemistry in harvested rLOX-PP tumors, but not in controls. Data provide pre-clinical findings that support proof of principle for the therapeutic anti-cancer potential of rLOX-PP protein formulations.

Citation: Bais MV, Nugent MA, Stephens DN, Sume SS, Kirsch KH, et al. (2012) Recombinant Lysyl Oxidase Propeptide Protein Inhibits Growth and Promotes Apoptosis of Pre-Existing Murine Breast Cancer Xenografts. PLoS ONE 7(2): e31188. doi:10.1371/journal.pone.0031188

Editor: Surinder K. Batra, University of Nebraska Medical Center, United States of America

Received July 15, 2011; **Accepted** January 3, 2012; **Published** February 8, 2012

Funding: This research was supported by NIH grants: R01 DE14066, RO1 CA82742, and R01 HL088572, and Department of Defense Idea Award W81XWH-08-1-0349 PC073646. The funders had no role in the study design, data collection and analysis, decision to publish, or preparation of the manuscript.

Competing Interests: The authors have declared that no competing interests exist.

* E-mail: trackman@bu.edu

Introduction

Lysyl oxidase (LOX) is a copper-dependent, extracellular matrix enzyme required for the normal biosynthesis of mature and functional collagens and elastin [1]. LOX is made as a 50 kDa proenzyme and processed extracellularly to a ~30 kDa mature LOX enzyme and the ~18 kDa propeptide (LOX-PP) by procollagen C-proteinases [2], encoded by the *bone morphogenetic protein-1* and the *tolloid-like-1* and *-2* genes [3,4]. The *LOX* gene has been shown to have "RAS rescission" activity, and this tumor suppressor activity of the *LOX* gene has been mapped to its propeptide region [5]. Natural and recombinant LOX-PP has N- and O-linked carbohydrates and a very high isoelectric point. The characterization of purified recombinant LOX-PP (rLOX-PP) showed that it is a highly disordered protein and is, therefore, predicted to have multiple binding partners and more than one mechanism of action [6].

LOX enzyme activity has been reported to promote tumor invasiveness [7,8]. LOX enzyme and LOX-PP are derived from the same mRNA, as summarized above. Interestingly, estrogen receptor positive breast cancer tumors are less invasive than estrogen receptor negative tumors, and express lower levels of LOX mRNA [9]. Taken together, data suggest a model in which abnormally low levels of LOX-PP may permit tumor growth, whereas abnormally high LOX enzyme may promote tumor invasion. Our interest here is to investigate the potential of rLOX-PP protein to inhibit tumor growth in vivo.

LOX-PP inhibits *RAS*-dependent transformation of NIH 3T3 fibroblasts assessed by inhibition of cell proliferation, growth in soft agar and Akt- and Erk1/2 dependent induction of NF-kappaB in vitro [5]. In breast cancer, LOX-PP was shown to reverse the invasive phenotype of Her2/neu driven breast cancer cells, inhibit epithelial to mesenchymal transition, and inhibit migration and branching colony formation. Retrovirus mediated ectopic overexpression of LOX-PP in NF639 cells suppresses xenograft tumor formation in nude mice [10]. In human lung and pancreatic cancer cells, LOX-PP reduces migration, Erk1/2 and Akt signaling, and growth in soft agar and represses BCL-2 levels [11]. Doxorubicin is a chemotherapeutic drug which induces apoptosis in cancer cells. Pre-treatment of pancreatic and breast cancer cells with rLOX-PP sensitizes the cancer cells to doxorubicin-induced apoptosis in vitro, whereas LOX-PP alone did not appear to induce apoptosis [12]. LOX-PP inhibits different signaling pathways. LOX-PP reduces tyrosine phosphorylated

FAK and p130^{cas} protein, and reduces haptotaxis of NF639, MDA-MB-231 and Hs578T breast cancer cells and thus attenuates fibronectin mediated integrin signaling [13]. rLOX-PP inhibits FGF-2 induced DNA synthesis, Erk1/2 and Akt signaling and FRS2alpha activation in DU145 prostate cancer cells and in the phenotypically normal MC3T3-E1 osteoblastic cell line [14,15]. Interestingly, the single nucleotide Arg158G polymorphism in a carboxy-terminal conserved region results in loss of some of the LOX-PP tumor suppressor properties [9], while some intracellular mechanisms of action depend on the amino-terminal end [16]. Taken together, the various studies have shown that LOX-PP has a tumor suppressor property, inhibits RAS, FGF-2, and FAK signaling, and that different conserved regions mediate its activity.

These studies strongly suggest that LOX-PP could have potential as a cancer therapeutic. The major goal of this study was to evaluate the ability of rLOX-PP protein to inhibit or reverse the growth of pre-existing breast cancer xenografts, first by direct intratumoral injection (i.t.); and second, by a slow release formulation in order to establish proof of principle that rLOX-PP protein formulations can have the potential as an in vivo cancer therapeutic. In order to gain insights into the mode of action of rLOX-PP protein in vivo, the effect on breast cancer xenograft cell proliferation and apoptosis was determined. Moreover, data suggest that LOX-PP protein persists in tumors particularly when administered by a slow release formulation in vivo. These findings support the notion that formulations of rLOX-PP may ultimately prove to have therapeutic utility in cancer therapy.

Materials and Methods

Cell line and Mouse xenograft model

The mouse mammary tumor virus (MMTV)-Her-2/neu NF639 cell line kindly provided by Dr. P. Leder [17] was grown in DMEM supplemented with 10% FBS. All experiments were performed as approved by Boston University Medical Center IACUC. In both experiments, the single cell suspensions in DMEM were prepared. NF639 cells (4×10^6 cells) were injected subcutaneously into the midline dorsa (n = 10/condition) of NCR nu/nu mice (Charles River Laboratories), and tumors allowed to grow to 100 mm^3. Caliper measurements were made at intervals to monitor the volume of all tumors.

Intratumoral injection

Purified rLOX-PP (10 micrograms) expressed by HEK293 cells [6] in PBS or PBS alone (vehicle) was injected once per day i.t. for 5 days starting on day 17 when the average tumor volume was 100 mm^3. Mice were monitored and maintained until day 21 at which time the PBS injected control tumors reached 1000 mm^3.

rLOX-PP slow release formulation in alginate beads

Alginate beads containing rLOX-PP and empty control beads were made according to a standard protocol [18] as follows. rLOX-PP (1 mg/ml) [6] and 18 mg/ml sodium alginate were mixed at a ratio of 1:2 and the slurry was passed drop-wise through a 21 gauge needle into a solution of $CaCl_2$ (1.5% w/v) with gentle mixing. Mixing was continued for five minutes, and then beads were allowed to settle for 10 minutes. Beads were washed three times in sterile water and stored in 150 mM NaCl, 1 mM $CaCl_2$ at 4°C until used. LOX-PP incorporation within the beads was calculated based on a 70% incorporation efficiency measured previously with other growth factors of similar size and molecular properties [19,20]. Empty beads were made without addition of rLOX-PP. Bead size was measured with a digital caliper (Fisher Scientific) and an average diameter of 1.50±0.12 mm (n = 20) was noted. Animal studies were conducted with a single preparation of beads to avoid batch to batch variability.

rLOX-PP in vitro release kinetics from LOX-PP/alginate beads

rLOX-PP release kinetics from calcium alginate beads were determined in vitro over a 14 day period. Three beads containing 1 μg rLOX-PP each were incubated in 1 ml release buffer (150 mM NaCl, 1 mM $CaCl_2$, 0.05% gelatin) with n = 4 at 37°C with constant shaking. The supernatant was collected on days 0, 1, 3, 7, 10 and 14. At each time point, the entire supernatant was removed and replenished with 1 ml fresh release buffer. Samples were boiled in 1X SDS PAGE sample buffer and aliquots were subjected to Western blot analysis, and compared to standard curves of rLOX-PP determined from the same blots after densitometric analyses and linear regression with the aid of a Versadoc densitometer and Quantity One software (BioRad). Total cumulative rLOX-PP released was then calculated.

In vivo implantation of rLOX-PP alginate beads

NF639 cells (4×10^6) were injected once in the dorsum of each mouse and tumors were allowed to grow to 300 mm^3 (n = 10/group). Then, 35 micrograms rLOX-PP in beads, or empty alginate beads (n = 10) were surgically implanted adjacent to each experimental and control tumor, respectively, on lateral sides of tumor borders and subsequently sutured with vicryl 4.0 biodegradable sutures. Tumor volumes were monitored by caliper measurements made at regular intervals, and tumor weights were determined at sacrifice.

Histology and immunohistochemistry

All tumors were harvested at sacrifice and then fixed in 4% paraformaldehyde for three hours, and then placed in 30% sucrose overnight at 4°C. Frozen sections were made and subjected to immunohistochemistry and quantitative histomorphometric analyses [21]. Four tumors, 3 to 4 sections per tumor, were used for immunohistochemistry staining analysis for the proliferation marker, Ki-67 (Abcam Inc.; ab15580), phospho-histone H3 (Millipore; 06-570), the apoptosis marker active caspase 3 (Trevigen, Gaithersburg, MD, USA; 2305-PC-020), and LOX-PP itself (Novus, NB110-41568). Apoptosis was further evaluated using a kit for the terminal deoxynucleotidyl transferase dUTP nick end labeling (TUNEL) assay according to the manufacturer's instructions (Trevigen, Gaithersburg, MD, USA; 4815-30-K) [22]. Quantitation of micrographs was performed independently by two experienced researches MB and SSS) in a blinded fashion according to previous protocols performed by this laboratory [21,23,24]. Five independent 0.09 mm^2 grids on three sections per animal were measured; a minimum of three mice per group was analyzed as indicated for each assay.

Western blotting

Snap frozen tumors were ground to a fine powder in liquid nitrogen and then extracted into SDS PAGE sample buffer (0.1 mM Tris-HCl, 4% SDS, 10% glycerol, 5% β-mercaptoethanol). Protein concentrations were determined using Nano Orange assay kits (Molecular Probes, Eugene, OR, USA). Approximately 10 micrograms of protein from 3 tumors per experimental group were then subjected to 10% SDS PAGE and Western blotting with primary antibodies for mitosis marker phospho-histone H3 (Millipore, Billerica, MA, USA; 06-570), the downstream targets of Ras signaling phospho-Erk1/2, total Erk1/2, and normalization

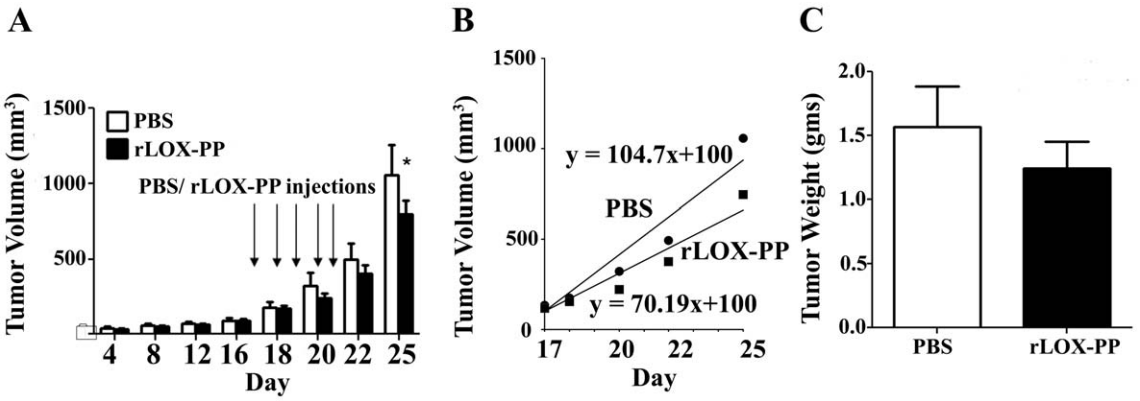

Figure 1. Injection of rLOX-PP inhibits NF639 xenograft growth in mice. (A) Subcutaneous xenografts of NF639 breast cancer cells were injected once daily with 10 micrograms rLOX-PP for 5 days beginning on day 17 (arrows). Tumor volumes were monitored by caliper measurements (n = 10; *, $p<0.05$); (B) The tumor growth rates were determined from measurements made beginning on day 18 and were derived from linear regression analyses of the data. (C) Tumor weights at sacrifice on day 25 (p = 0.4, n = 10).
doi:10.1371/journal.pone.0031188.g001

control beta-actin (Cell Signaling, Danvers, MA, USA; antibodies 9101S, 9102S and 4970L, respectively). Anti-rabbit secondary antibodies were purchased from Cell Signaling Technology (Danvers, MA, USA; 7074S). The quantifications were performed by a digital densitometry system and Quantity One software (Versadoc; BioRad, Eugene, OR, USA).

Statistics

Analyses of all experiments were done using two way ANOVA with Bonferroni post-hoc analysis or Student's *t*-test (GraphPad Prism 5 software). Data are presented as means +/− SD.

Results

Intratumoral injection of rLOX-PP inhibits pre-existing breast cancer xenografts

Earlier studies have shown that the ectopic expression of LOX-PP inhibits breast and pancreatic cancer xenograft growth, and proliferation of prostate cancer cells in vitro [10,12,14]. To evaluate whether rLOX-PP protein can inhibit the growth of preexisting tumors in vivo, we used a breast cancer xenograft model. NF639 breast cancer cells (4×10^6 cells) were injected subcutaneously into the dorsal region of nude mice and tumors allowed to grow to a volume of 100 mm^3 (day 17). Mice were then divided randomly into two groups with 10 mice each. Mice were injected once per day beginning on day 17 for five consecutive days with 10 micrograms rLOX-PP or vehicle (PBS) in a volume of 100 microliters. Caliper measurements were continued through day 25 at which time tumors injected with vehicle (controls) reached a volume of 1000 mm^3. Data in Figure 1A show that on day 25 the average tumor volume in the rLOX-PP i.t. injection group was 743 ± 101 mm^3 compared with PBS control (1043 ± 199 mm^3) showing significantly inhibited tumor growth in LOX-PP treated tumors ($p\leq0.05$). The growth rate was plotted from the tumor volume measurements beginning on day 18. The growth rate in the vehicle group was 125 mm^3 per day compared to 85 mm^3 per day in rLOX-PP treated tumors (Figure 1B). Consistent with the above findings, the tumor weights determined at sacrifice were smaller in the rLOX-PP injected group (Figure 1C) but not significantly different from control (p = 0.41). Thus, the data show that i.t. injection of rLOX-PP significantly inhibits the tumor volume growth by 28% on day 25 and growth rate by 32% after day 18 compared to PBS, and a trend toward diminished tumor weight was found.

Sustained release of rLOX-PP

To evaluate whether rLOX-PP could be stabilized for slow and sustained release and provide enhanced stability and possibly increased biological activity in vivo, we incorporated rLOX-PP into alginate beads. Alginate is a naturally occurring aquatic plant polysaccharide polymer and alginate beads have been used previously for successful slow release of FGF-2 and other proteins with high isoelectric points without loss of biological activity [18,25]. rLOX-PP is also a highly basic protein with a high isoelectric point [6]. In order to determine whether rLOX-PP can be released from alginate beads in a time-dependent manner, in vitro release kinetics were determined as outlined in Materials and Methods. Data in Figure 2 indicate that rLOX-PP is released

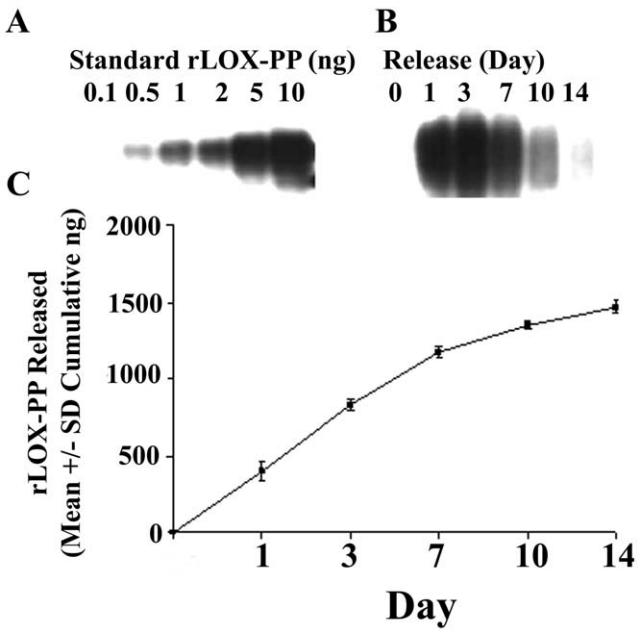

Figure 2. Alginate bead release kinetics of rLOX-PP. (A) Western blot of known amounts of rLOX-PP ranging from 0.1 to 10 ng of rLOX-PP; (B) Western blot of rLOX-PP-bead supernatants collected at different intervals; (C) calculated cumulative release of rLOX-PP; (n = 4; *, $p<0.001$).
doi:10.1371/journal.pone.0031188.g002

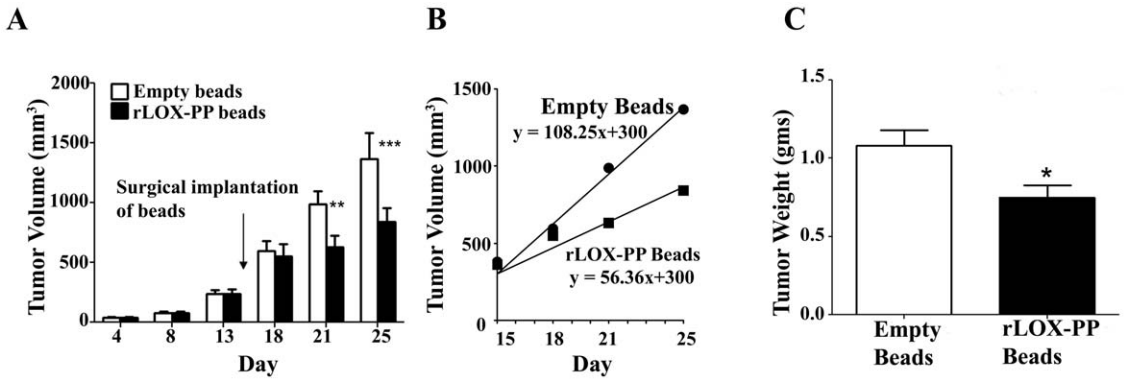

Figure 3. rLOX-PP incorporated in alginate beads inhibits NF639 xenograft growth in mice compared to empty beads. (A) Subcutaneous 100 mm^3 xenografts of NF639 breast cancer cells were established in mice. rLOX-PP/alginate or empty beads were implanted on day 15 (arrow). Tumors were monitored by caliper measurements (n = 10; *, $p<0.05$, ***, $p<0.01$). (B) The tumor growth rates were determined from measurements made beginning on day 18 and were derived from linear regression analyses of the data; (C) tumor weights determined at sacrifice on day 25 (n = 10; *, $p<0.05$).
doi:10.1371/journal.pone.0031188.g003

continuously over the experimental period of 14 days ($p \leq 0.001$) with apparent linear release between day 1 and day 7 (Figure 2B), slowing after day 7 (Figure 2C). In total, 50% of rLOX-PP encapsulated in alginate beads was released into buffer by day 14 (Figure 2C) with the remainder still bound to alginate. In vivo, tightly bound LOX-PP would potentially be released because alginate is progressively resorbed [26].

To determine the activity of rLOX-PP/alginate beads to effectively inhibit breast cancer xenograft growth we first established NF639 tumors as described in Materials and Methods. Empty alginate beads or beads containing a total of 35 micrograms rLOX-PP were then implanted adjacent to the xenografts through a small incision made on each of two sides of the tumor. rLOX-PP/alginate beads significantly inhibited tumor growth

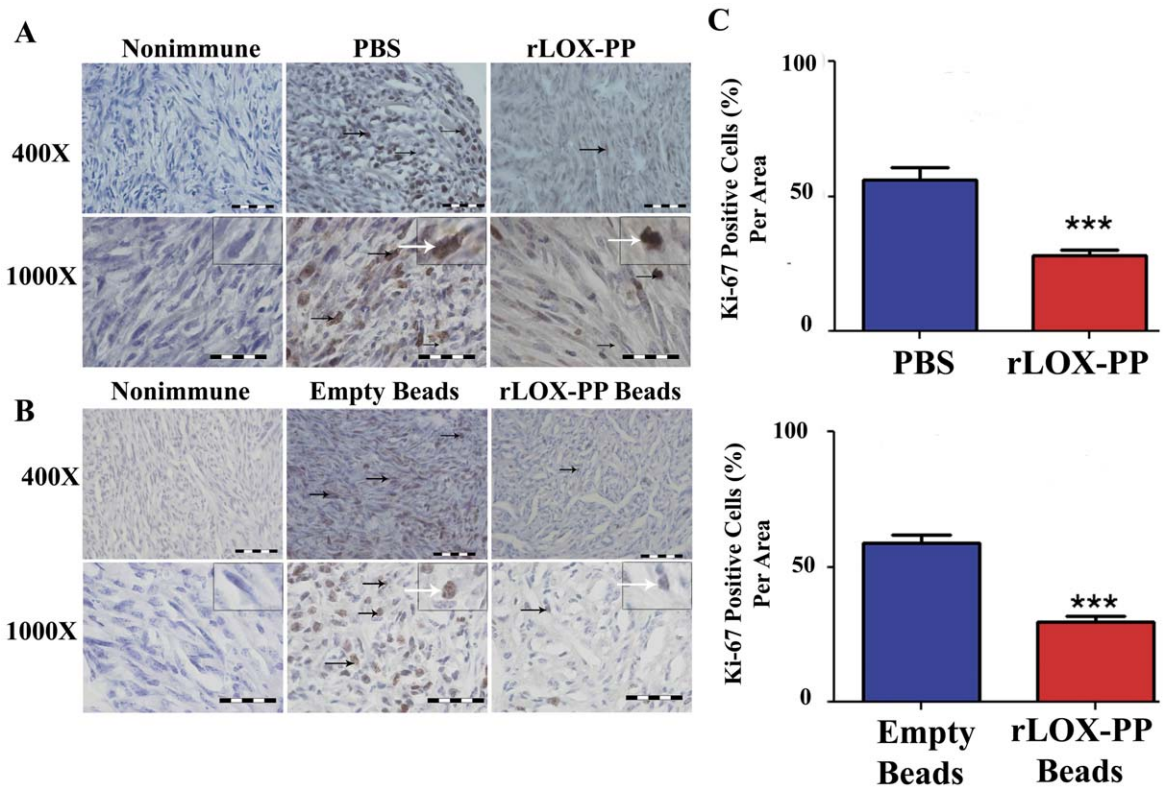

Figure 4. Proliferation marker Ki-67 is decreased by rLOX-PP treatment. (A) Immunostaining with Ki-67 antibody or non-immune IgG control tumors after (A) direct i.t. injection of rLOX-PP compared to PBS and (B) after implantation of empty and rLOX-PP alginate beads. Black arrows mark some positive-stained cells; the white arrows point to an inset containing an enlarged image of a stained cell. (C) The corresponding quantifications are shown (***, $p<0.001$; n = 3). Scale bar = 0.005 mm.
doi:10.1371/journal.pone.0031188.g004

compared to empty beads on day 21 and 25 (Figure 3A). Tumor size in animals implanted with rLOX-PP were 7%, 36% and 38% lower on days 18, 21, and 25, respectively, compared to control mice. The tumor growth rate was determined by plotting tumor volumes beginning on day 18 and revealed a rate of 110 mm^3/day for control tumors (empty beads) compared to 42 mm^3/day for the rLOX-PP treated tumors (rLOX-PP/alginate beads), demonstrating a 61% reduction in growth rate after rLOX-PP bead implantation adjacent to tumor xenografts (Figure 3B). The final average tumor weight at sacrifice was 30% lower after rLOX-PP/alginate bead implantation (Figure 3C). In summary, data indicate that rLOX-PP/alginate bead implantation resulted in lower final tumor volume by 38% on day 25, 30% lower final tumor weight, and a 61% lower tumor growth. Taken together, findings show that both i.t. injection of rLOX-PP and slow release formulations of rLOX-PP effectively inhibit NF639 xenograft growth. In addition, it is apparent that a lower amount of rLOX-PP (35 micrograms) when administered in a slow release formulation is more effective at inhibiting tumor growth than i.t. injection of a higher total amount of rLOX-PP (a total of 50 micrograms: 10 micrograms per day as described above).

rLOX-PP inhibits tumor growth by reducing proliferation and increasing apoptosis

In order to gain insights into mechanisms by which LOX-PP inhibits tumor growth in vivo, we first evaluated relative expression levels of Ki-67 by immunohistochemistry in harvested tumors. Ki-67 is a marker for cell proliferation, and is expressed in all phases of the cell cycle except G_0, and is a predictive and prognostic marker for breast cancer [27,28,29,30,31]. A higher number of Ki-67 immunopositive cells were observed in sections injected with PBS or implanted with empty beads compared to rLOX-PP injection or rLOX-PP/alginate beads implantation, as seen in representative sections (Figure 4A and 4B). The proportion of Ki-67 immunopositive cells was reduced by both direct i.t. injection of rLOX-PP and rLOX-PP/alginate beads compared to their respective controls (Figure 4C; $p<0.001$). In addition, histone H3 is phosphorylated specifically during mitosis and is also frequently used as a proliferation marker in cancer. Both Ki-67 and phosphorylated histone H3 have been used for identification of aggressive human breast and ovarian cancer and positively correlate with the tumor grade [32,33]. Data in Figure 5A and 5B suggest the presence of a reduced number of phospho-histone H3 stained cells in both direct i.t. injection of rLOX-PP and rLOX-PP/alginate bead treated tumors compared to their respective controls. The quantitation of phospho-histone H3 from tumor tissue protein extracts by Western blotting showed an average reduction of 45–50% in both i.t. injection of LOX-PP (Figure 5C; $p<0.05$) and rLOX-PP/alginate beads (Figure 5D; $p<0.05$). Thus, direct i.t. injection of rLOX-PP and rLOX-PP/alginate beads each respectively reduced Ki-67 and phospho-histone H3 by approximately 50% in this breast cancer xenograft model.

Apoptosis is induced by at least two different pathways: death receptor (extrinsic) and mitochondrial (intrinsic) pathways. Both

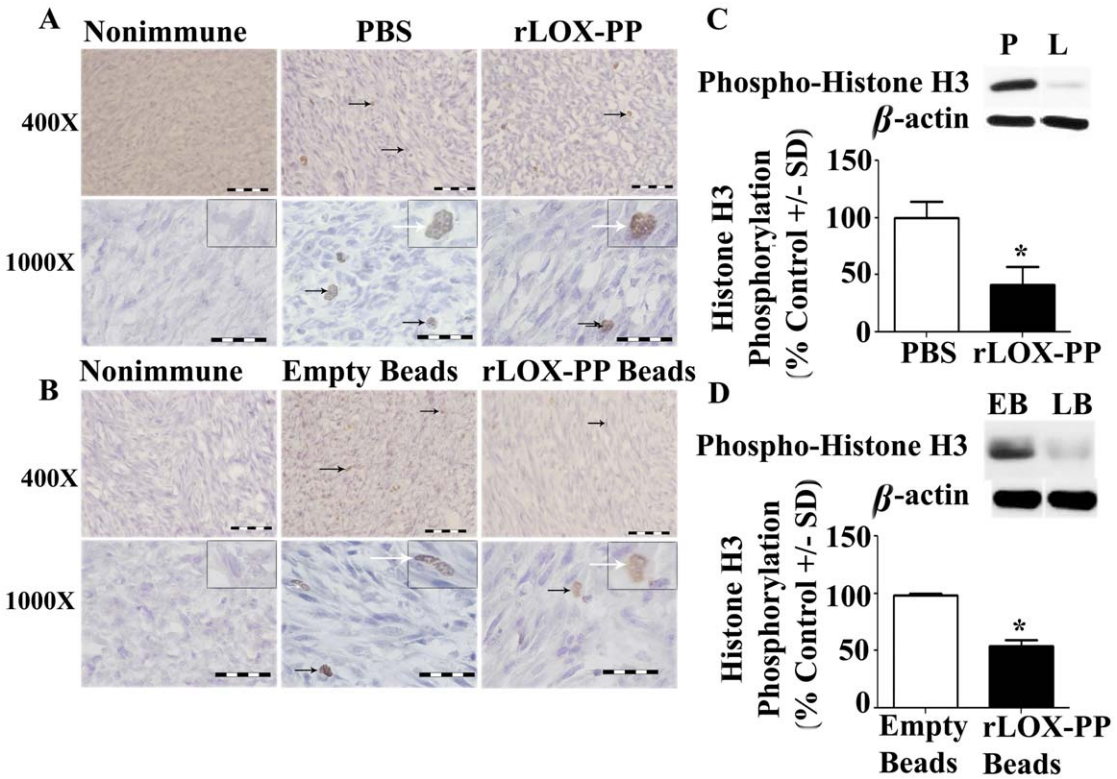

Figure 5. Proliferation marker phosphorylated histone H3 is decreased by rLOX-PP treatment. (A) Immunostaining with phospho-histone H3 antibody or nonimmune IgG control tumors after (A) direct i.t. injection of rLOX-PP (L) compared to PBS (P) and (B) after implantation of empty (EB) and rLOX-PP (LB) alginate beads. Black arrows mark some positive-stained cells; the white arrows point to an inset containing an enlarged image of a stained cell. Scale bars correspond to 0.005 mm for 400× and 0.002 mm for 1000×. Arrows mark some positively stained cells. (C) Western blot analyses of 17 kDa phospho- histone H3, 36 kDa beta-actin and the corresponding quantifications of protein extracts from tumors after (C) direct i.t. injections of rLOX-PP compared to PBS and (D) after implantation of empty and rLOX-PP alginate beads (*, $p<0.01$; $n=3$).
doi:10.1371/journal.pone.0031188.g005

pathways converge at caspase 3 activation that can be detected by immunohistochemistry. Representative micrographs (Figures 6A and 6B) and quantitative scoring of all data (Figure 6C) suggest that both i.t. injection and slow release of rLOX-PP increased the number of cells staining for active cleaved caspase-3 in breast cancer xenografts.

To determine more directly whether apoptosis and DNA fragmentation were enhanced by rLOX-PP, we performed TUNEL assays as indicated in Materials and Methods. TUNEL positive cells (Figure 7A and B) were found to be significantly increased to about 10% of cells in sections with rLOX-PP i.t. injection or rLOX-PP/alginate beads, compared to about 2% for controls (Figure 7C; $p<0.0001$). Taken together with activated caspase 3 measurements shown in Figure 6, the data indicate that rLOX-PP inhibits proliferation and stimulates apoptosis in breast cancer xenografts.

We next investigated whether LOX-PP itself could be detected in harvested tumors using a specific anti-LOX-PP antibody in immunohistochemistry assays [34]. As seen in Figure 8, data indicate that rLOX-PP is easily detected at elevated levels in tumors from mice implanted with rLOX-PP alginate beads compared to empty beads. By contrast, although the same trend is observed in tumors derived from direct i.t. injection experiments, the level of detectable rLOX-PP appears to be less than for rLOX-PP/alginate.

We next evaluated a downstream target of Ras signaling to ask whether the mechanism of rLOX-PP protein in vivo is likely to occur by mechanisms that we have described in vitro and in ectopic expression studies both in vitro and in vivo. Figure 9 shows that Erk1/2 phosphorylation was inhibited by more than 70% after rLOX-PP i.t. injections (Figure 9A) and rLOX-PP/alginate slow release (Figure 9B) compared to respective controls. Thus, data are consistent with findings that rLOX-PP protein functions by inhibiting Ras signaling in a pre-clinical breast cancer xenograft model.

Discussion

Here we show for the first time that rLOX-PP protein inhibits pre-existing tumor growth after direct i.t. injection or when applied in a slow release formulation. Intratumoral injection studies have been classically done in initial studies to evaluate the ability of proteins to inhibit tumor growth. Direct i.t. injection of tumor necrosis factor-alpha and interferons, or interferons alone, were shown to inhibit xenograft growth in mice [35,36,37]. In human patients, i.t. injection of recombinant IL-2 induced tumor killing, tumor necrosis and lymphocytic infiltration [38]. Thus, consistent with other pre-clinical and clinical studies, it is here shown that direct i.t. injection of rLOX-PP inhibited the growth of a pre-existing breast cancer xenograft. Interestingly, the slow release formulation appeared to be more effective than i.t. injection of naked rLOX-PP in the inhibition of NF639 xenograft growth. Although, LOX-PP has been shown to have tumor suppressor properties, the effectiveness of rLOX-PP protein to inhibit pre-existing tumor growth has not been previously evaluated in vivo. Such studies are important in the evaluation of therapeutic potential.

Alginate beads have been used previously for successful slow release of recombinant proteins with a high isoelectric point

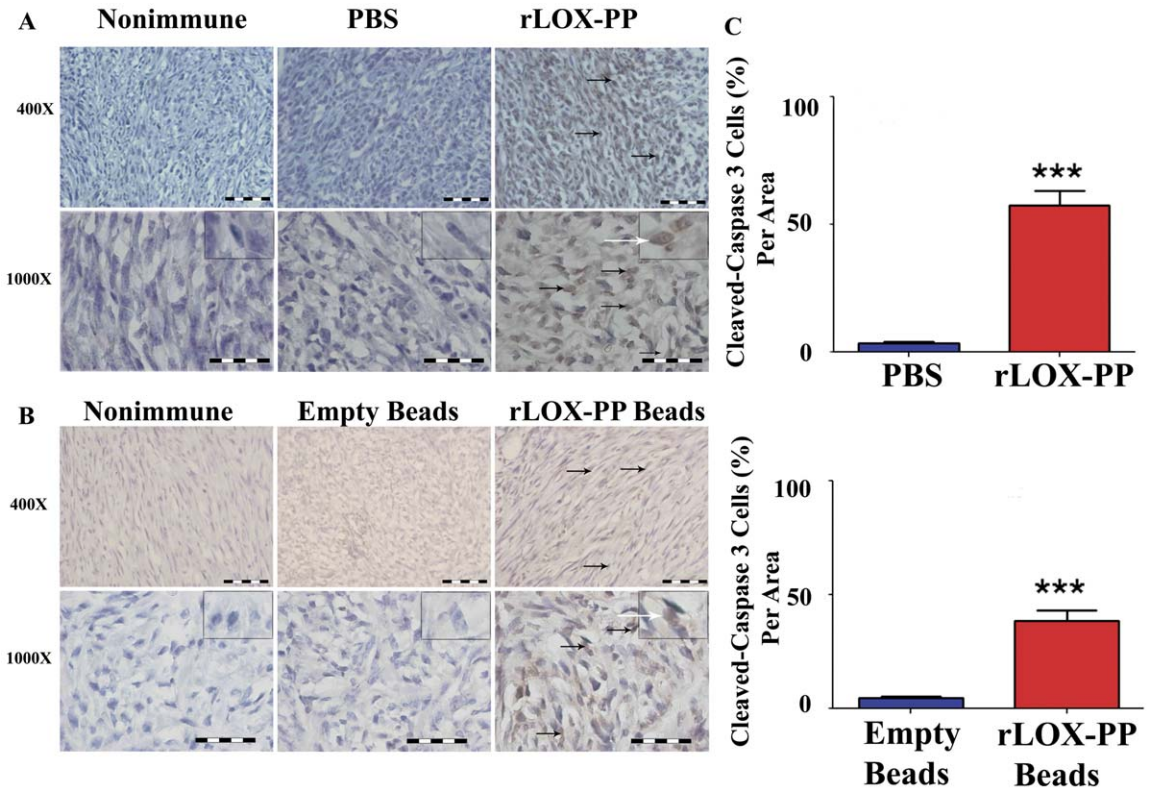

Figure 6. Apoptosis marker active caspase 3 is increased by rLOX-PP treatment. (A) Immunostaining of tumors with active caspase 3 antibody, or non-immune IgG control. (A) i.t. rLOX-PP- or PBS injected tumors, and (B) tumors treated with surgically implanted empty alginate beads or rLOX-PP/alginate beads. Black arrows mark some positive-stained cells; the white arrows point to an inset containing an enlarged image of a stained cell. Scale bar = 0.005 mm for 400× and 0.002 mm for 1000×; (C) the corresponding quantifications (***, $p<0.001$; n = 3).
doi:10.1371/journal.pone.0031188.g006

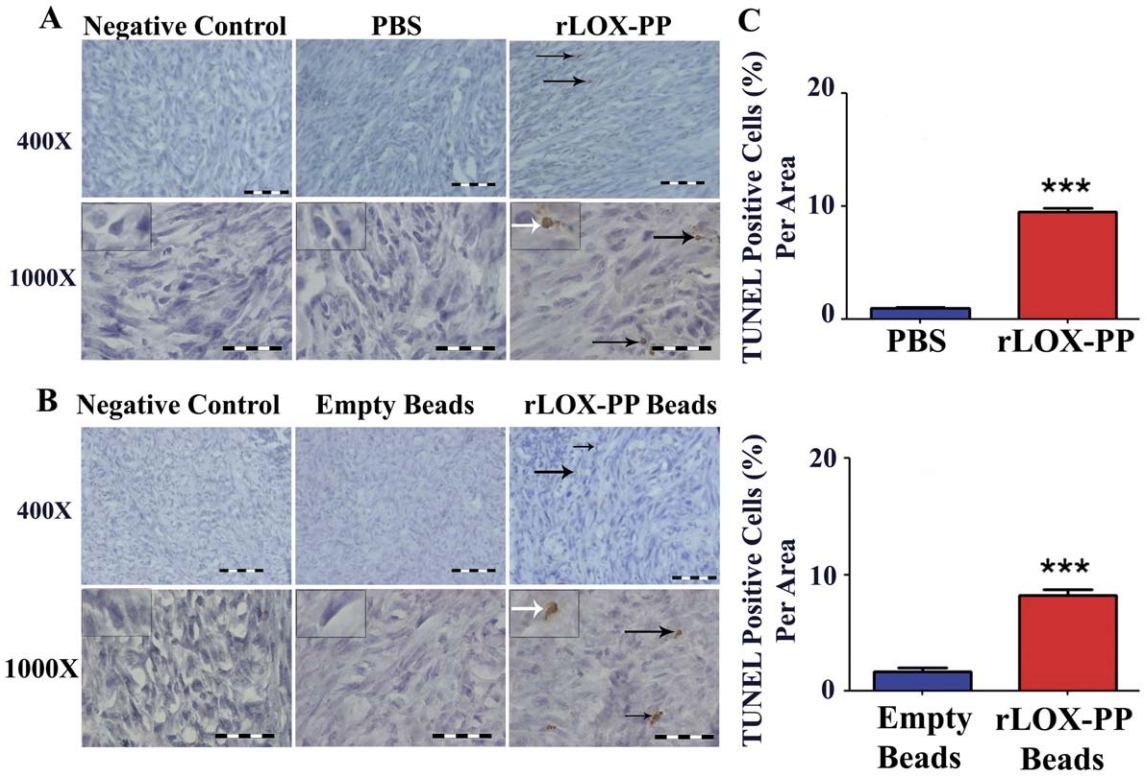

Figure 7. Apoptosis marker TUNEL is increased by rLOX-PP treatment. (A) TUNEL staining of tumors treated i.t. with rLOX-PP, or tumors injected with negative control PBS; (B) tumors treated with surgically implanted empty alginate beads or rLOX-PP alginate beads. Black arrows mark some positive-stained cells; the white arrows point to an inset containing an enlarged image of a stained cell. Scale bar = 0.005 mm for 400× and 0.002 mm for 1000×; (C) the corresponding quantifications (***, $p<0.001$; n = 3). Arrows mark some positive-stained cells.
doi:10.1371/journal.pone.0031188.g007

without loss of biological activity [18,25]. In human clinical studies, alginate beads containing human mature allogenic chondrocytes were found to be an effective treatment for cartilage defects in the knee showing significant improvement within six months which shows that alginate is safe and feasible for application in vivo in patients [39]. Alginate formulations, therefore, could have potential for use in pre-clinical human studies, although other carriers such as polylactide/polyglycolide polymers may be more widely used [40]. Encapsulated proteins in alginate beads are released by diffusion from and degradation of

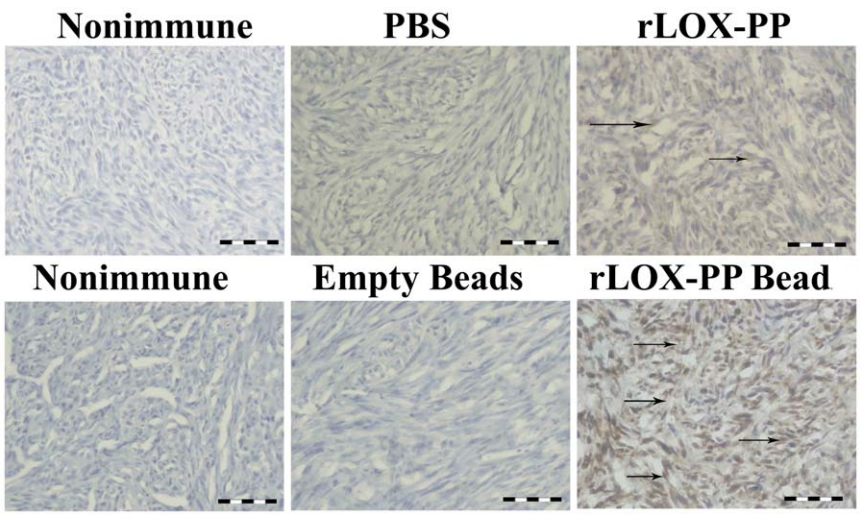

Figure 8. rLOX-PP persists in treated tumors. Immunostaining of tumors after sacrifice with LOX-PP antibody or non-immune IgG control from mice after (A) direct i.t. injection of rLOX-PP compared to PBS or (B) after implantation of empty or rLOX-PP-containing alginate beads. Scale bars = 0.005 mm. Arrows mark some positive-stained cells.
doi:10.1371/journal.pone.0031188.g008

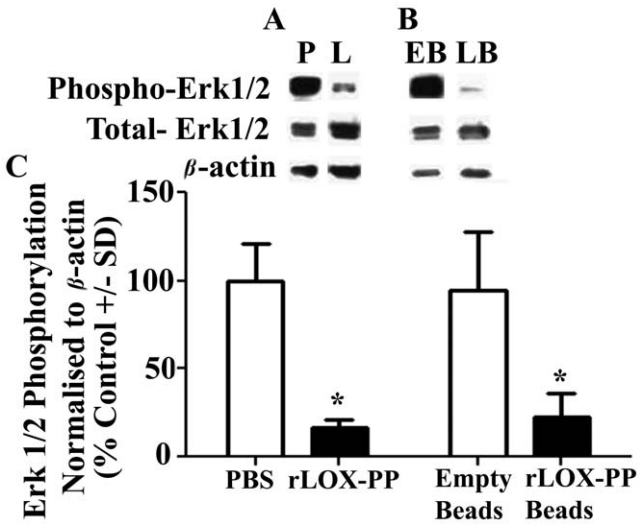

Figure 9. LOX-PP inhibits Ras effector Erk1/2 phosphorylation in vivo. Western blot analysis of 42 and 44 kDa phospho-Erk, total Erk1/2 and 36 kDa beta-actin from tumor extracts after (A) direct i.t. injections of rLOX-PP (L) compared to PBS (P); (B) after implantation of empty (EB) and rLOX-PP (LB) alginate beads; (C) the corresponding quantifications are shown (*, $p<0.05$; $n=3$).
doi:10.1371/journal.pone.0031188.g009

alginate beads for in vivo applications [41], and the present study is significant in that it provides proof of principle that rLOX-PP is effective in vivo, especially in a slow release formulation. At sacrifice, it was apparent that most of the bead material had been resorbed in all implanted mice, as expected. Only 1–2 beads out of the twelve beads implanted per mouse could be found at sacrifice (data not shown) suggesting that more than 80% of rLOX-PP was released in vivo.

The single implantation of alginate incorporated rLOX-PP is more efficient than five i.t. injections of rLOX-PP. The total amount of rLOX-PP incorporated in alginate beads was 35 micrograms and resulted in a more significant reduction in tumor xenograft volume, growth rate and tumor weight compared to 50 micrograms rLOX-PP direct i.t. injections over five days. Similarly, other studies have shown that alginate encapsulation of recombinant proteins are highly active in vivo. For example, similar to our data with rLOX-PP, in vivo subcutaneous implantation of a single dose of alginate beads containing IL-17R was more effective in reducing inflammation when compared to multiple subcutaneous injections of this anti-inflammatory protein [41]. FGF-2 plays an important role in tissue repair and has a very short half-life when administered parenterally. Surgical implantation of FGF-2 bound to heparin-Sepharose beads encapsulated in calcium alginate microcapsules in an arterial injury model was more efficient in delivering FGF-2 within the arterial wall when compared to intravenous administration [18]. Thus, consistent with other studies, rLOX-PP inhibits tumor xenograft by direct i.t. injection or implantation of alginate encapsulated rLOX-PP, yet the latter shows a stronger effect with an apparently increased persistence of rLOX-PP in tumors as seen in Figure 6. Although there are many possibilities to improve the current formulation of rLOX-PP for in vivo application, the current formulation of alginate beads with encapsulated rLOX-PP inhibited tumor growth rate by more than 61% and provides proof of principle that rLOX-PP protein in some form has therapeutic potential. It now becomes of considerable interest to determine the pharmacokinetics, pharmacodynamics, and stability and effectiveness of systemically applied naked rLOX-PP and of protected formulations of rLOX-PP that would be acceptable for human trials in order to develop rLOX-PP as an anti-cancer drug candidate.

In order to investigate mechanisms of inhibition, we evaluated effects of rLOX-PP on cell proliferation and apoptosis. rLOX-PP inhibits cell proliferation determined by reduced expression of two independent proliferation markers: Ki-67 and phospho-histone H3. Ki-67 has been used to evaluate the responsiveness of chemotherapeutics to breast cancer patients and evaluate the risk of tumor incidence after treatments [42,43]. Ki-67 has diagnostic importance in distinguishing between benign and malignant tumors [44,45,46], and is a prognostic factor for clinical breast cancer patients [47,48,49]. Phospho-histone H3 has been similarly employed to evaluate tumor grade and aggressiveness [32,33]. Phospho-histone H3 is a prognostic proliferation marker in triple negative invasive lymph node-negative breast cancer [50].

Data further show that rLOX-PP induces apoptosis in breast cancer xenografts which was evaluated by activated caspase 3 immunostaining and TUNEL assays. Apoptosis is induced by different pathways which converge at caspase 3 activation, a pro-apoptotic marker [51]. Recently, it has been shown that rLOX-PP sensitizes pancreatic and breast cancer cells to doxorubicin induced apoptosis in vitro [12], but whether rLOX-PP alone could induce apoptosis in breast cancer xenografts in vivo was not known. The mechanism by which rLOX-PP induces apoptosis of cancer cells in vivo in the absence of other chemotherapeutic agents as seen in the present study requires further evaluations. The NCR nu/nu mouse model employed in the present study is T-cell deficient, but contains natural killer (NK) cells and B cells. It is, therefore, possible to speculate that the increased apoptosis observed in rLOX-PP treated tumors in vivo could be driven by enhanced sensitivity to NK cell-derived TRAIL, or FasL stimulated signaling [52,53]. A greater understanding of molecular mechanisms of action of LOX-PP may permit the design of combinatorial therapeutic approaches that would be more effective than individual chemotherapeutic approaches. As noted, it is of interest that rLOX-PP inhibits tumor growth in vivo characterized by inhibition of cell proliferation and induction of apoptosis, whereas in vitro rLOX-PP alone inhibits proliferation but has not been seen to promote apoptosis [12].

Earlier in vitro studies done with ectopic rLOX-PP expression in cancer cell lines indicate that LOX-PP inhibits Ras-mediated activation of Erk1/2 by inhibiting FGF-2 to FGFR1 receptor binding and activation, and by direct interaction with Hsp70 and c-Raf [14,15,16]. The current study extends these observations to rLOX-PP protein administered in vivo in which we show highly significant inhibition of Erk1/2 phosphorylation. It is likely that mechanisms of LOX-PP identified primarily in vitro are operative in vivo, but further study of individual molecular interactions in vivo with wild type and mutant forms of rLOX-PP will be required to investigate the relationship between specific molecular interactions and actual inhibition of tumor growth. The observation of similarities in the magnitudes of rLOX-PP administration on altering levels of both proliferation and apoptosis markers, whereas tumor inhibition is more pronounced in the slow release model is likely to be coincidental. Without more continuous assays of changes in the expression of these markers throughout the entire experimental period, it is difficult to comment further. Importantly, the current study establishes experimental systems by which a variety of questions can now be addressed in vivo.

In conclusion, rLOX-PP protein is effective in inhibiting mouse xenograft growth. The data show that alginate bound rLOX-PP is more efficient in inhibiting breast cancer xenograft compared to

direct i.t injections. Further understanding of the mechanisms by which rLOX-PP inhibits breast cancer xenograft growth will enhance the ability to design potentially more effective combinations of anti-cancer regimens.

Author Contributions

Conceived and designed the experiments: PCT MVB MAN. Performed the experiments: MVB SSS DNS MAN. Analyzed the data: MVB PCT GES KHK. Contributed reagents/materials/analysis tools: MVB SSS DNS MAN KHK. Wrote the paper: MVB PCT. All authors critically reviewed and approved the manuscript.

References

1. Kagan HM, Trackman PC (1991) Properties and function of lysyl oxidase. Am J Respir Cell Mol Biol 5: 206–210.
2. Cronshaw AD, Fothergill-Gilmore LA, Hulmes DJ (1995) The proteolytic processing site of the precursor of lysyl oxidase. Biochem J 306(Pt 1): 279–284.
3. Kessler E, Takahara K, Biniaminov L, Brusel M, Greenspan DS (1996) Bone morphogenetic protein-1: the type I procollagen C-proteinase. Science 271: 360–362.
4. Uzel MI, Scott IC, Babakhanlou-Chase H, Palamakumbura AH, Pappano WN, et al. (2001) Multiple bone morphogenetic protein 1-related mammalian metalloproteinases process pro-lysyl oxidase at the correct physiological site and control lysyl oxidase activation in mouse embryo fibroblast cultures. J Biol Chem 276: 22537–22543.
5. Palamakumbura AH, Jeay S, Guo Y, Pischon N, Sommer P, et al. (2004) The propeptide domain of lysyl oxidase induces phenotypic reversion of ras-transformed cells. J Biol Chem 279: 40593–40600.
6. Vora SR, Guo Y, Stephens DN, Salih E, Vu ED, et al. (2010) Characterization of recombinant lysyl oxidase propeptide. Biochemistry 49: 2962–2972.
7. Bondareva A, Downey CM, Ayres F, Liu W, Boyd SK, et al. (2009) The lysyl oxidase inhibitor, beta-aminopropionitrile, diminishes the metastatic colonization potential of circulating breast cancer cells. PloS One 4: e5620.
8. Erler JT, Bennewith KL, Nicolau M, Dornhofer N, Kong C, et al. (2006) Lysyl oxidase is essential for hypoxia-induced metastasis. Nature 440: 1222–1226.
9. Min C, Yu Z, Kirsch KH, Zhao Y, Vora SR, et al. (2009) A loss-of-function polymorphism in the propeptide domain of the LOX gene and breast cancer. Cancer Res 69: 6685–6693.
10. Min C, Kirsch KH, Zhao Y, Jeay S, Palamakumbura AH, et al. (2007) The tumor suppressor activity of the lysyl oxidase propeptide reverses the invasive phenotype of Her-2/neu-driven breast cancer. Cancer Res 67: 1105–1112.
11. Wu M, Min C, Wang X, Yu Z, Kirsch KH, et al. (2007) Repression of BCL2 by the tumor suppressor activity of the lysyl oxidase propeptide inhibits transformed phenotype of lung and pancreatic cancer cells. Cancer Res 67: 6278–6285.
12. Min C, Zhao Y, Romagnoli M, Trackman PC, Sonenshein GE, et al. (2010) Lysyl oxidase propeptide sensitizes pancreatic and breast cancer cells to doxorubicin-induced apoptosis. J Cell Biochem 111: 1160–1168.
13. Zhao Y, Min C, Vora SR, Trackman PC, Sonenshein GE, et al. (2009) The lysyl oxidase pro-peptide attenuates fibronectin-mediated activation of focal adhesion kinase and p130Cas in breast cancer cells. J Biol Chem 284: 1385–1393.
14. Palamakumbura AH, Vora SR, Nugent MA, Kirsch KH, Sonenshein GE, et al. (2009) Lysyl oxidase propeptide inhibits prostate cancer cell growth by mechanisms that target FGF-2-cell binding and signaling. Oncogene 28: 3390–3400.
15. Vora SR, Palamakumbura AH, Mitsi M, Guo Y, Pischon N, et al. (2010) Lysyl oxidase propeptide inhibits FGF-2-induced signaling and proliferation of osteoblasts. J Biol Chem 285: 7384–7393.
16. Sato S, Trackman PC, Maki JM, Myllyharju J, Kirsch KH, et al. (2011) The Ras signaling inhibitor LOX-PP interacts with Hsp70 and c-Raf to reduce Erk activation and transformed phenotype of breast cancer cells. Molecular and Cellular Biology 31: 2683–2695.
17. Elson A, Leder P (1995) Protein-tyrosine phosphatase epsilon. An isoform specifically expressed in mouse mammary tumors initiated by v-Ha-ras OR neu. J Biol Chem 270: 26116–26122.
18. Edelman ER, Nugent MA, Karnovsky MJ (1993) Perivascular and intravenous administration of basic fibroblast growth factor: vascular and solid organ deposition. Proc Natl Acad Sci U S A 90: 1513–1517.
19. Nehra A, Gettman MT, Nugent M, Bostwick DG, Barrett DM, et al. (1999) Transforming growth factor-beta1 (TGF-beta1) is sufficient to induce fibrosis of rabbit corpus cavernosum in vivo. The Journal of Urology 162: 910–915.
20. Nugent MA, Langer R, Chen O, Edelman ER (1992) Controlled release of fibroblast growth factor: Activity in cell culture. Mater Res Soc Symp Proceed 252: 273–284.
21. Uzel MI, Kantarci A, Hong HH, Uygur C, Sheff MC, et al. (2001) Connective tissue growth factor in drug-induced gingival overgrowth. J Periodontol 72: 921–931.
22. Kantarci A, Augustin P, Firatli E, Sheff MC, Hasturk H, et al. (2007) Apoptosis in gingival overgrowth tissues. J Dent Res 86: 888–892.
23. Kantarci A, Black SA, Xydas CE, Murawel P, Uchida Y, et al. (2006) Epithelial and connective tissue cell CTGF/CCN2 expression in gingival fibrosis. J Pathol 210: 59–66.
24. Sume SS, Kantarci A, Lee A, Hasturk H, Trackman PC (2010) Epithelial to mesenchymal transition in gingival overgrowth. Am J Pathol 177: 208–218.
25. Edelman ER, Nugent MA, Smith LT, Karnovsky MJ (1992) Basic fibroblast growth factor enhances the coupling of intimal hyperplasia and proliferation of vasa vasorum in injured rat arteries. J Clin Invest 89: 465–473.
26. Kaul G, Cucchiarini M, Arntzen D, Zurakowski D, Menger MD, et al. (2006) Local stimulation of articular cartilage repair by transplantation of encapsulated chondrocytes overexpressing human fibroblast growth factor 2 (FGF-2) in vivo. J Gene Med 8: 100–111.
27. Colozza M, Sidoni A, Piccart-Gebhart M (2004) Value of Ki67 in breast cancer: the debate is still open. Lancet Oncol 11: 414–415.
28. Santisteban M, Reynolds C, Barr Fritcher EG, Frost MH, Vierkant RA, et al. (2010) Ki67: a time-varying biomarker of risk of breast cancer in atypical hyperplasia. Breast Cancer Research and Treatment 121: 431–437.
29. Tanei T, Shimomura A, Shimazu K, Nakayama T, Kim SJ, et al. (2011) Prognostic significance of Ki67 index after neoadjuvant chemotherapy in breast cancer. European journal of surgical oncology: Journal of the European Society of Surgical Oncology and the British Association of Surgical Oncology 37: 155–161.
30. Ueda S, Tsuda H, Saeki T, Omata J, Osaki A, et al. (2011) Early metabolic response to neoadjuvant letrozole, measured by FDG PET/CT, is correlated with a decrease in the Ki67 labeling index in patients with hormone receptor-positive primary breast cancer: a pilot study. Breast Cancer 18: 299–308.
31. Yerushalmi R, Woods R, Ravdin PM, Hayes MM, Gelmon KA (2010) Ki67 in breast cancer: prognostic and predictive potential. The Lancet Oncology 11: 174–183.
32. Aune G, Stunes AK, Tingulstad S, Salvesen O, Syversen U, et al. (2011) The proliferation markers Ki-67/MIB-1, phosphohistone H3, and survivin may contribute in the identification of aggressive ovarian carcinomas. International Journal of Clinical and Experimental Pathology 4: 444–453.
33. Bossard C, Jarry A, Colombeix C, Bach-Ngohou K, Moreau A, et al. (2006) Phosphohistone H3 labelling for histoprognostic grading of breast adenocarcinomas and computer-assisted determination of mitotic index. J Clin Pathol 59: 706–710.
34. Hurtado PA, Vora S, Sume SS, Yang D, St Hilaire C, et al. (2008) Lysyl oxidase propeptide inhibits smooth muscle cell signaling and proliferation. Biochem Biophys Res Commun 366: 156–161.
35. Ozzello L, Habif DV, De Rosa CM, Cantell K (1988) Treatment of human breast cancer xenografts using natural interferons-alpha and -gamma injected singly or in combination. J Interferon Res 8: 679–690.
36. Balkwill FR, Lee A, Aldam G, Moodie E, Thomas JA, et al. (1986) Human tumor xenografts treated with recombinant human tumor necrosis factor alone or in combination with interferons. Cancer Res 46: 3990–3993.
37. Ozzello L, Habif DV, De Rosa CM, Cantell K (1988) Effects of intralesional injections of interferons-alpha on xenografts of human mammary carcinoma cells (BT20 and MCF-7). J Interferon Res 8: 207–215.
38. Shirai M, Watanabe S, Nishioka M (1990) Antitumour effect of intratumoral injection of human recombinant interleukin-2 in patients with hepatocellular carcinoma: a preliminary report. Eur J Cancer 26: 1045–1048.
39. Almqvist KF, Dhollander AA, Verdonk PC, Forsyth R, Verdonk R, et al. (2009) Treatment of cartilage defects in the knee using alginate beads containing human mature allogenic chondrocytes. Am J Sports Med 37: 1920–1929.
40. Santana RB, Trackman PC (2006) Controlled release of fibroblast growth factor 2 stimulates bone healing in an animal model of diabetes mellitus. Int J Oral Maxillofac Implants 21: 711–718.
41. Wee S, Gombotz WR (1998) Protein release from alginate matrices. Adv Drug Deliv Rev 31: 267–285.
42. Nishimura R, Osako T, Okumura Y, Hayashi M, Arima N. Clinical significance of Ki-67 in neoadjuvant chemotherapy for primary breast cancer as a predictor for chemosensitivity and for prognosis. Breast Cancer 17: 269–275.
43. Guarneri V, Piacentini F, Ficarra G, Frassoldati A, D'Amico R, et al. (2009) A prognostic model based on nodal status and Ki-67 predicts the risk of recurrence and death in breast cancer patients with residual disease after preoperative chemotherapy. Ann Oncol 20: 1193–1198.
44. Petrovic D, Babic D, Forko JI, Martinac I. Expression of Ki-67, P53 and progesterone receptors in uterine smooth muscle tumors. Diagnostic value. Coll Antropol 34: 93–97.
45. Yu L, Wang L, Zhong J, Chen S. Diagnostic value of p16INK4A, Ki-67, and human papillomavirus L1 capsid protein immunochemical staining on cell blocks from residual liquid-based gynecologic cytology specimens. Cancer Cytopathol 118: 47–55.
46. Taheri ZM, Mehrafza M, Mohammadi F, Khoddami M, Bahadori M, et al. (2008) The diagnostic value of Ki-67 and repp86 in distinguishing between benign and malignant mesothelial proliferations. Arch Pathol Lab Med 132: 694–697.
47. Wiesner FG, Magener A, Fasching PA, Wesse J, Bani MR, et al. (2009) Ki-67 as a prognostic molecular marker in routine clinical use in breast cancer patients. Breast 18: 135–141.

48. de Azambuja E, Cardoso F, de Castro G, Jr., Colozza M, Mano MS, et al. (2007) Ki-67 as prognostic marker in early breast cancer: a meta-analysis of published studies involving 12,155 patients. Br J Cancer 96: 1504–1513.
49. Mohsenifar J, Almassi-Aghdam M, Mohammad-Taheri Z, Zare K, Jafari B, et al. (2007) Prognostic values of proliferative markers ki-67 and repp86 in breast cancer. Arch Iran Med 10: 27–31.
50. Skaland I, Janssen EA, Gudlaugsson E, Hui Ru Guo L, Baak JP (2009) The prognostic value of the proliferation marker phosphohistone H3 (PPH3) in luminal, basal-like and triple negative phenotype invasive lymph node-negative breast cancer. Cellular Oncology 31: 261–271.
51. Andersen MH, Becker JC, Straten P (2005) Regulators of apoptosis: suitable targets for immune therapy of cancer. Nat Rev Drug Discov 4: 399–409.
52. Menke C, Goncharov T, Qamar L, Korch C, Ford HL, et al. (2011) TRAIL receptor signaling regulation of chemosensitivity in vivo but not in vitro. PloS One 6: e14527.
53. Screpanti V, Wallin RP, Grandien A, Ljunggren HG (2005) Impact of FASL-induced apoptosis in the elimination of tumor cells by NK cells. Molecular Immunology 42: 495–499.